

Characterization Of Pavement Surface Texture Using 3D Laser Scanner Technique

G. Dondi, A. Simone, V. Vignali & C. Lantieri
DISTART, University of Bologna, Bologna, Italy (www.distart.unibo.it)

ABSTRACT: Characterization of surface texture is very important for pavement management applications, because it can affect road characteristics and vehicle performance in the areas of tire wear, rolling resistance, tire and road friction, noise in vehicles, exterior road noise and discomfort.

Many of the pavement texture measurement devices reduce the data to a single attribute such as mean profile depth or hydraulic radius. Although mean profile depth was correlated with friction and noise, it is not the only contributing factor. Texture size, spacing and distribution should also be considered. Therefore, advanced methods that characterize pavement texture in three dimensions are needed.

In this paper the authors proposed a 3D laser scanner system for recovering pavement surface macrotexture. To analyze its potentialities, the results obtained on different pavement types were compared with traditional measured texture profiles.

KEY WORDS: Surface texture, laser scanner, road materials, road noise

1. INTRODUCTION

Road surface texture is defined as deviation of actual surface from an ideal reference plane. Surface texture is composed by two elements:

- micro-texture, constituted by wavelength values inferior to 0.5 mm and profile peak-to-peak width values between 1 μm and 0.2 mm, which is the result of roughness of individual aggregate items used in road surface material and is therefore tightly connected to the mineralogical composition of an aggregate;
- macro-texture, constituted by wavelength and peak-to-peak width values between 0.5 mm and 50 mm and 0.2 mm and 10 mm, respectively, depending on mixture size range and laying and tamping procedures, being the result of intergranular mixture.

Texture is vital to road safety, since it is a main factor in road evenness, water draining, tire-road grip and tire vibrations. An accurate survey is thus evidently important.

To such purpose, the potential of a laser-scan 3-D technique is examined in this paper for the detection of road pavement macro- and micro-texture.

2. EQUIPMENT USED

2.1 Instruments

NEXTENGINE 3D Laser Scanner, a desktop laser scanner for short-distance and small objects deploys the MultiStripe Laser Triangulation (MLT) technology in order to consolidate data coming from four light blades (Matija et al. 2008).

Triangulation laser devices such as the device used are based on forward intersection topographical principle and are therefore able to determine the position of one point within the instrumental reference system space. In particular, it is provided with:

- an emitting source allowing to scan the reference area by rotating at α emission angle;
- a reception sensor acquiring the ray reflected from surface at β reflection angle, determining the point coordinates at a given distance.

In addition to geometrical data, the instrument also allows to catch radiometric data. Its 3 MP CMOS sensor allows obtaining colour information from scanned surfaces. Integrated illuminators ensure objects are properly lit up during image acquisition. The device allows operating at Macro and Wide operating modes, differing in terms of accuracy, working distance and scanning surface size on one object (table 1) (Guidi et al. 2007).

Table 1: Laser scanner technical specifications and operating modes

	Macro	Wide
Scan area	13x10 cm	35x25 cm
Scan distance	18 cm	40 cm
Accuracy	127 μ m	381 μ m
Point density	200 DPI	75 DPI
Texture resolution	400 DPI	150 DPI

Acquisition speed is about 50,000 points/sec with an average delay of 90 seconds for each scan. Regarding use-related biological risks, the scanner is provided with 4 solid-state laser emitters with 650 nm wavelength, class 1M (fully safe operations except when rays are widened through magnification factor lenses).

2.2 Data acquisition and processing

Have been scanned several samples, measured about 15 cm in diameter and represented different types of coarse surfaces: a conventional coarse surface, a SMA coarse surface and a draining coarse surface (figure 1).

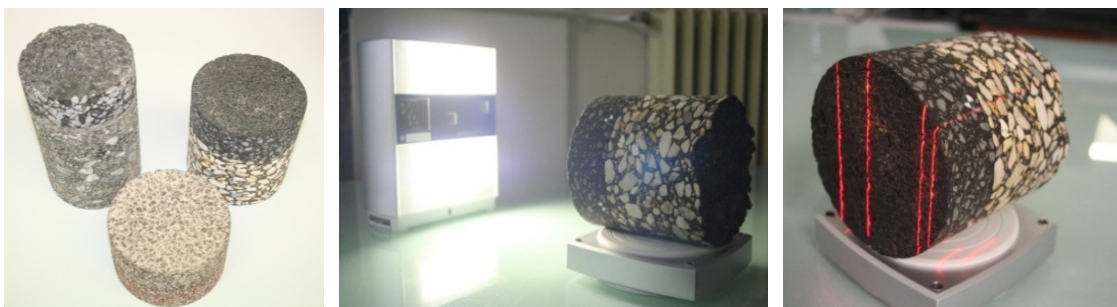


Figure 1: Scanned samples

Laser datum acquisition was performed in both Macro and Wide modes. The scanner was set for individual scans at the best quality available, with an acquisition delay time of 120 sec approximately. In order to acquire an image of the whole surface with a single scan, samples were placed at about 40 cm when scanned in Wide mode. Since the acquisition size in Macro mode was smaller, four scans were required for SMA and draining coarse samples, and 6 scans were required for the conventional coarse surface in order to acquire the whole surface of every sample (figure 2).



Figure 2: Scan organisation in conventional coarse surface

Scan data were user-filtered in order to remove both image portions of sample stands and any outliers, that is rough mistakes in point determination. Mesh objects obtained were exported as *.obj and were linked to a single local reference system. Once aligned, they have been consolidated in a single mesh object describing the whole sample surface. In order to do so, redundant points were removed along with triangulation faults resulting from:

- “non manifold” mesh conditions (3 surfaces are in the same side) (figure 3, no. 1);
- Overlapping faces (some sides intersect) (figure 3, no. 2);
- Face redundancy (figure 3, no. 3);
- Inverted mesh normal (figure 3, no. 4).

A final DSM (Digital Surface Model) is obtained representing sample orography (figure 3, no. 5).

In order to determine which data acquisition system would better suit the exam application, surfaces obtained through Wide and Macro modes (figures 4 and 5) were compared along with the relevant deviations for each analysed sample. Surface results obtained in Wide mode were subtracted to those obtained with Macro mode (figures 6 and 7).

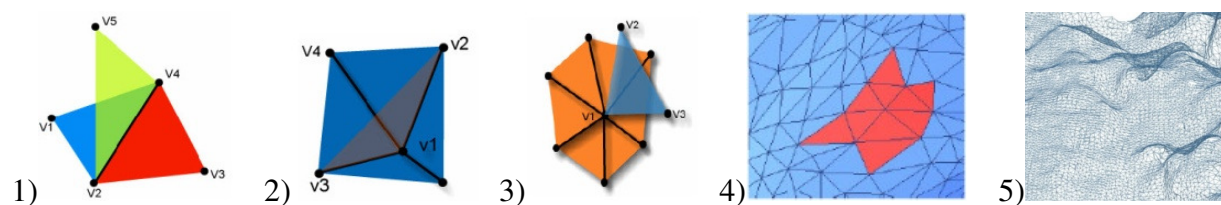


Figure 3. Triangulation faults and wireframe surface representation

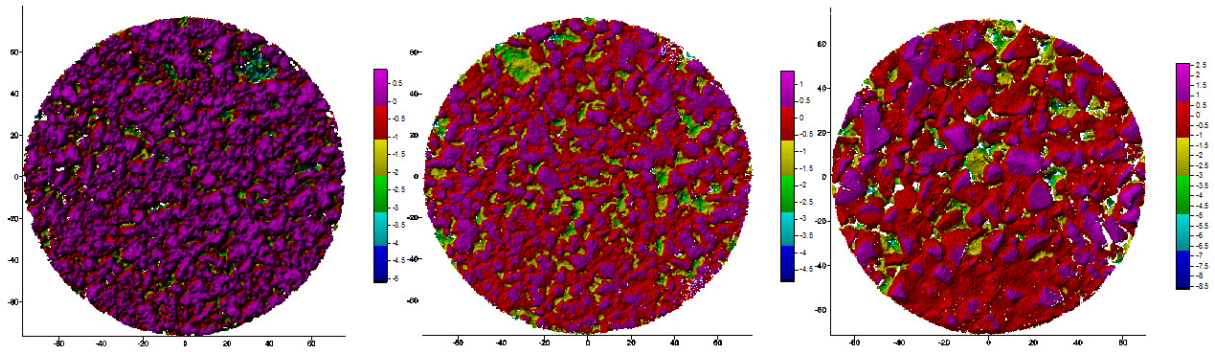


Figure 4: Wear, SMA and draining surfaces scanned with MACRO mode

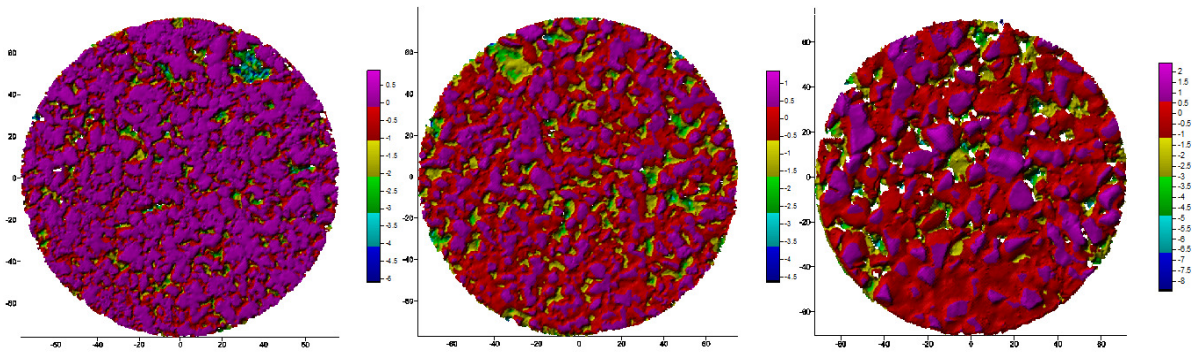


Figure 5: Wear, SMA and draining surfaces scanned with WIDE mode

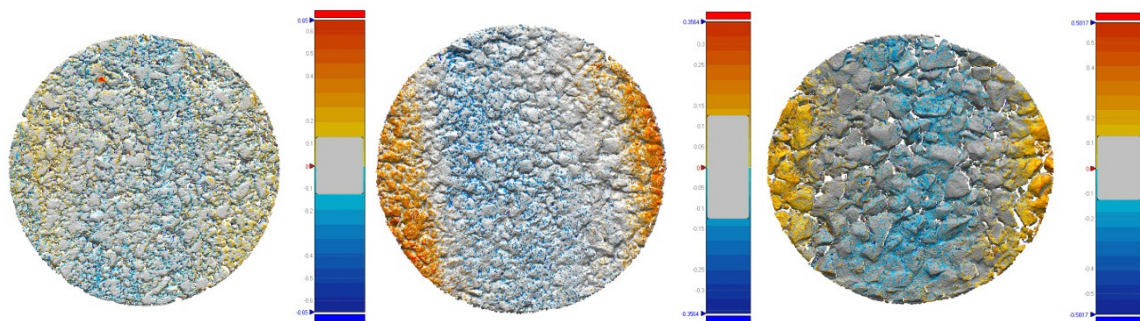


Figure 6: Deviations from Macro and Wide shells for all three samples (Wear, SMA, Draining)

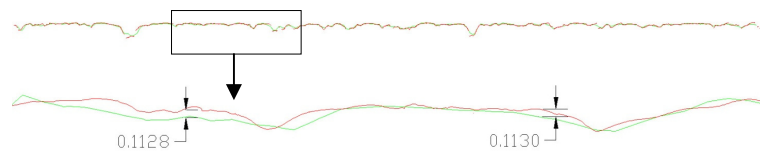


Figure 7: Deviations between Macro (red) and Wide (green) modes

One may notice that deviations between surfaces are comprised in an assumed tolerance range of $127\ \mu\text{m}$ throughout most of the sample. Such value corresponds to maximum

instrumental accuracy.

Wide operating mode therefore allows to obtain a morphologically representative image with one single scan, with a smaller number of dropouts, and processable with no particular mesh filtering operations. Opposite, the surface appears smoothed compared to Macro mode, since points spacing does not allow for a perfect detection of micro-roughness. For this reason, the application at issue was executed with Macro as the reference procedure.

3. CASE STUDY

3.1 Introduction

In order to assess its significance, results obtained through laser scanner were compared with indicators conventionally used in order to measure adherence (table 2) (Boscaino et al. 2000). In particular, the following indicators were considered:

- HS value, assessing surface roughness mean height as the between a given sand volume and the relevant covered area;
- Mean Profile Depth (MPD), determining profile mean depth as the difference between arithmetic mean of two peaks and mean level on a 100 mm baseline (UNI 13473-1:2004);
- average roughness (Ra), that is the average value of (absolute) deviations with reference to mean profile line (figure 8);
- peak to valley height (Rt), that is the maximum vertical distance between the highest peak value and the lowest profile valley (figure 8);
- levelling depth (Ru), that is the depth resulting from the distance between average line and a straight line tangential to the profile peak (figure 8);
- mean depth (Rm), that is the distance between average line and a parallel line tangential to the most accentuated cavity, that is the lowest point (figure 8).

The values of indicators chosen – to be considered valid for a given profile – have been evaluated again with the laser scanner in order to be exported in a 3-D environment. To such purpose, 8 profiles have been created for each sample by intersecting the mesh with adequate normal surfaces and rotated by 22.5° (figure 9). In this way, a simulation of profilometer has been obtained and parameters such as roughness and MPD (with a baseline equal to sample diameter) have been obtained on a 2-D basis to be compared against 3-D results (Ala. 2007).

Table 2: Texture indicators

Indicator	M.u.	Description	Class
MPD	[L]	Mean profile depth	Geometrical
Ra	[L]	Average roughness	
Ru	[L]	Levelling depth	
Rm	[L]	Mean depth	
Rp	[L]	Surface roughness depth	
Rt	[L]	Peak to valley height	
HS	[L]	Sand height	Performance related
BPN		Grip Number	
MTD	[L]	Mean Texture Depth	Statistical
VAR	[L ²]	Variance	
Rms	[L]	Average quadratic deviation	
Rsk		Skewness	
Rku		Kurtosis	

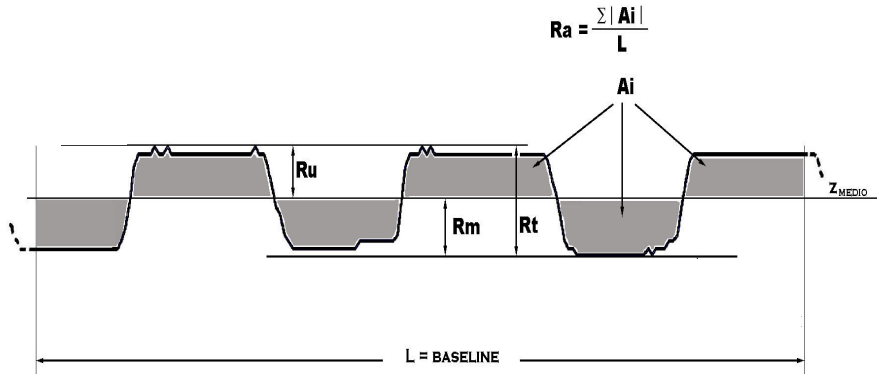


Figure 8: Indicators detected by means of profilometers

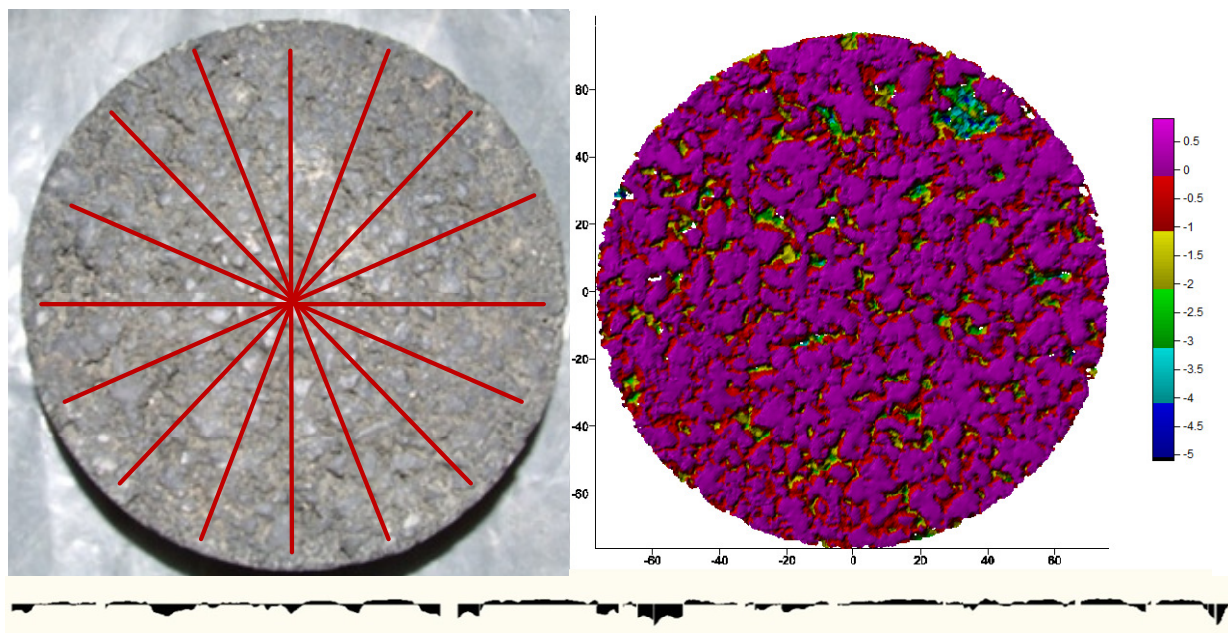


Figure 9: Section arrangement and reconstruction of their profile

3.2 Materials

The samples were chosen with a 15 cm diameter, representing different coarse surfaces: a conventional coarse surface, an SMA coarse surface and a draining coarse surface (figures 10 and 11). In particular, the relevant granulometric data are comprised in the data provided in the relevant technical specifications.



Figure 10: Conventional, SMA and draining samples

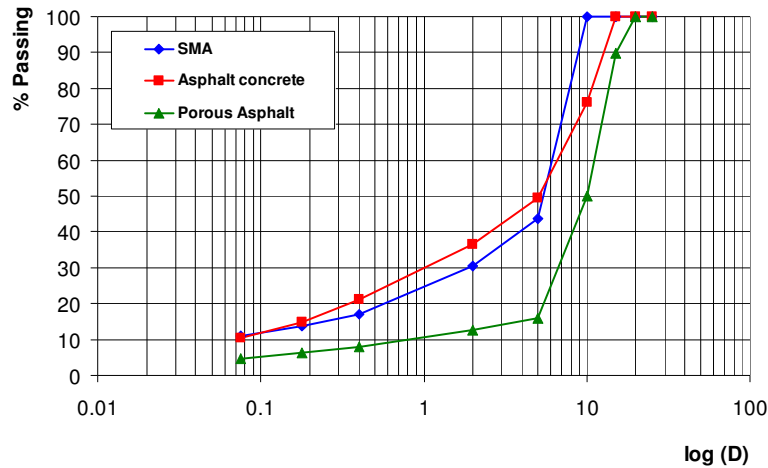


Figure 11: Granulometric range of examined samples

Table 3 illustrates samples specifications in order to qualify material and provide for on-site evidence by means of traditional adherence assessment tests.

Table 3. Specifications of examined samples

Sample	Bitumen [%]	Residue vacuum [%]	Diameter [mm]	Height [mm]	Weight [g]	HS [mm]	BPN
Wear	6.48	2	153.5	51.5	2220	0.64	63
SMA	6.90	7.5	153	44	1718	0.81	66
Draining	4.65	20.2	143	43	1419	1.57	64

3.3 Results

Table 4 shows results obtained.

Table 4: parameters describing roughness average height (8s means average of 8 sections)

Sample	$Ra' = V/A$ [mm]	Rt [mm]	Ru [mm]	Rm [mm]	HS [mm]	$Ra = A/L$ (8s) [mm]	MPD (8s) [mm]
Wear	0.46	6.13	1.02	-5.11	0.65	0.41	0.65
SMA	0.50	6.26	1.44	-4.86	0.81	0.51	0.97
Draining	0.80	11.22	2.58	-8.63	1.57	0.79	1.54

It can be seen that:

- in calculating roughness with Ra' (volume-surface ratio) and with average Ra (surface-length ratio) among the 8 sections described above does not show any particular deviation, when calculated along all samples points;
- MPD value – also calculated on 8 sections – shows max-min deviations of 20-35% among samples. The draining sample shows more significant deviations, indicating a more accentuated availability of peaks and valleys. A laser detection product allows to obtain an infinite number of profiles, allowing to obtain an MPD value tending to grow steady on actual value.
- when considering the same sample, MPD and HS values are very similar. This trend finds

an evidence in test operating modes: sand shaving on sample tends to conform at higher peaks, getting closer to mean profile depth represented by MPD.

Moreover, laser scanning allows to obtain coordinates for all detected points, in turn allowing to build histograms representing height distribution (figure 12). A higher number of points available on the sample representing conventional wear layer is a consequence of the higher number of scans performed.

Through histograms, one may obtain a global view of height distribution for the three samples, according to the following parameters (table 5):

- standard deviation, indicating height dispersion against average surface (expected value). A higher value thus represents a higher diversity in sizes;
- symmetry level index of distribution around its own average, for which negative values indicate a prevalence of valleys;
- Kurtosis parameter, constituting a measurement of a density function tail “thickness”, indicating range levelling value against normal distribution.

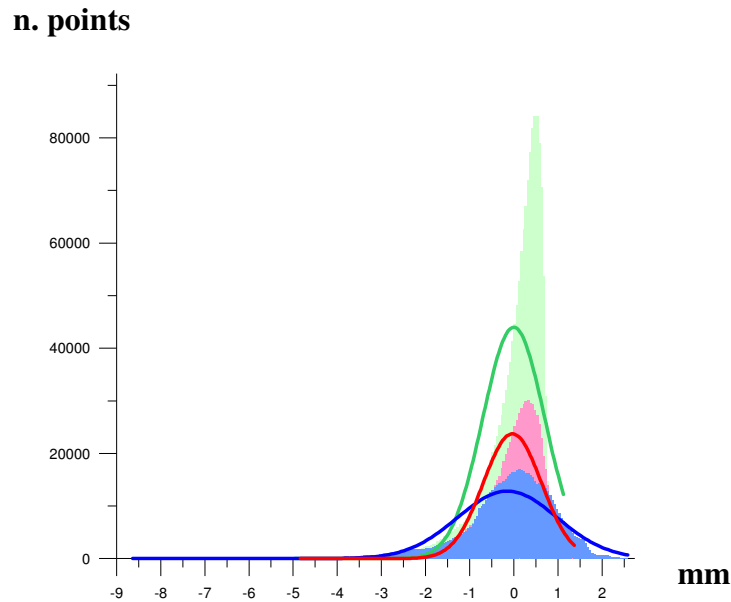


Figure 12: Height distribution with reference to mean surface for draining sample (blue), SMA sample (red), wear (green)

Table 5: Sample statistic parameters

Parameters	Wear	SMA	Draining
No. Of values	1550523	785611	726897
Min [mm]	-4.96	-4.84	-8.63
Max [mm]	1.15	1.40	2.58
Variance (VAR) [mm ²]	0.49	0.44	1.28
Standard deviation (Rms) [mm]	0.70	0.66	1.13
Skewness (Rsk)	-2.01	-1.20	-1.44
Kurtosis (Rku)	5.31	2.07	4.18

In particular, the Kurtosis value shows that draining and coarse surfaces are homogeneous within the sample despite the different materials, while SMA shows a diverse distribution determining a smaller Rku value.

With reference to the difference in samples texture, draining surface shows a greater variance due to a higher vacuum incidence - affecting the structure compactness. The high Rsk value in wear sample is probably due to a greater on-site compressing and therefore, a greater surface levelling.

Examined materials were also assessed in terms of water drainage on road surface, assuming that water layer is an even plane intersecting roughness and by recreating the emerged bitumen surface according to water volume increase on sample. In particular, the cutting surface has been varied by a 0.5 mm Δz range in order to simulate vacuum filling during rain (figure 13). The draining sample has a bigger capacity, as it includes almost a double water volume. At equal water volume values, it keeps a higher emerged surface value, thus increasing the tire-pavement surface and adherence accordingly. Individual draining features should also be taken into account, as they allow for different degrees of down flow.

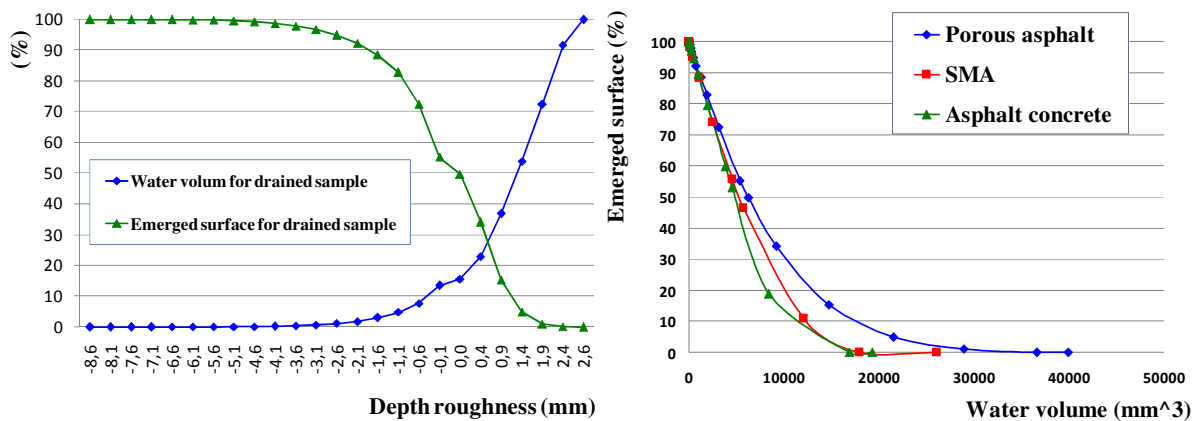


Figure 13: comparison between water volume-emerged area and behaviour with respect to roughness depth

In order to test the examination tool potentials in terms of ease and quickness of use, a SMA bituminous sample was analysed and the results of a single scan / four scans were compared (table 6).

An analysis of obtained results shows that both the number of acquired points and emerged area values increase with increasing scans, due to a reduction in gaps rates. Values so obtained, deviate from previous results by a 4 ÷ 9%.

Geometrical (surface) Ru and Rm indicator values also increase, though they are not as explicatory in reason of their absoluteness (not a mean value) (figure 14).

Statistic indicators size ranges varies slightly. This may also be seen in the shape of both distributions, which only vary in height given a different number of detected points. Detection based on four scans does not bring any additional elements to the single-scan survey.

In the light of future developments, it is important to set a range of values for each scanned indicator, in order to define the acceptability range for each material.

Table 6: SMA sample survey through one/four scans

	No. Of values	Rm	Ru	Variance (VAR) [mm ²]	Rsk	Rku	Emerged surface (mm ²)
4 scans	1232833	-6.697353	2.102654	0.8833521	-1.503	2.647	16243
1 scan	1132596	-5.699	1.8817	0.8071596	-1.492	2.297	15624

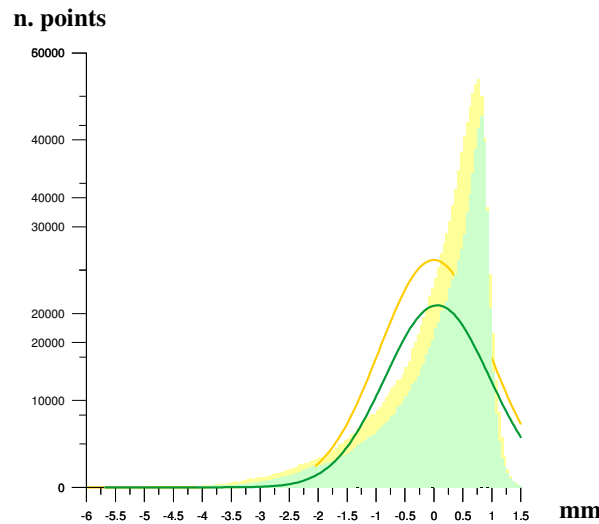


Figure 14: Height distribution with reference to mean plane, comparison with a single scan (green) and four scans (yellow).

4. CONCLUSIONS

Obtained results confirm 3D laser scanner potentials in detecting road surface texture patterns. In fact, this technique offers a 3D datum on surface course and thus implies several benefits both in monitoring mixture laying, and in case of on-site checks such as:

- volumetric and surface studies involving adherence and tire-pavement grip;
- on-site or log monitoring of pavement status in order to keep wear under control during surface life cycle;
- surface compressing level, through monitoring of macro-texture after treatment with tamping rollers.

5. REFERENCES

- Ala, A., M. Emin, K., Haleh, A. 2007. *Three-Dimensional Surface Texture Characterization of Portland Cement Concrete Pavements*. Computer-Aided Civil and Infrastructure Engineering.
- Boscaino, G., Minnella, I., Praticò, F.G., Vaiana, R., 2000. *L'analisi della tessitura stradale attraverso il sistema S.I.R.A.T.* X Convegno Nazionale SIV, Acireale, Catania;
- Guidi, G., Remondino, F., Morlando, G., Del Mastio, A., Ucheddu, F., Pelagotti, A., 2007. *Performance evaluation of a low cost active sensor for cultural heritage documentation*. VIII Conference on Optical 3D Measurement Techniques, Zurich, Switzerland;
- Matija, J., Matjaž, F., Janez, M., 2008. *Multiple Line Triangulation System for Real-time 3-D Monitoring of Chest Wall During Breathing*. Journal of Mechanical Engineering.